frontiers | Frontiers in Ecology and Evolution

ORIGINAL RESEARCH
published: 26 April 2022
doi: 10.3389/fevo.2022.897410

Effective Air Purification *via* Pt-Decorated N_3-CNT Adsorbent

Yinli Yang[1†], Sitong Liu[1†], Kai Guo[1], Liang Chen[1,2], Jing Xu[1] and Wei Liu[1*]*

[1] *Department of Optical Engineering, College of Optical, Mechanical and Electrical Engineering, Zhejiang A&F University, Hangzhou, China,* [2] *School of Physical Science and Technology, Ningbo University, Ningbo, China*

Effectively removal of air pollutants using adsorbents is one of the most important methods to purify the air. In this work, we proposed for the first time that PtN_3-CNT is an effective adsorbent for air purification. Its air purification performance was studied by calculating the adsorption behaviors and electronic structures of 12 gas molecules, including the main components of air (N_2, O_2, H_2O, CO_2) and the most common air pollutants (NO, NO_2, SO_3, SO_2, CO, O_3, NH_3, H_2S), on the surface of PtN_3-CNT using first-principles calculations. The results showed that these gases were adsorbed stably *via* the coordination between Pt and the coordinated atoms (C, N, O, and S atoms) in the gas molecules, and the adsorption energies vary in the range of −0.81∼−4.28 eV. The obvious chemical interactions between PtN_3-CNT and the adsorbed gas molecules are mainly determined by the apparent overlaps between the Pt *5d* orbitals and the outmost *p* orbitals of the coordination atoms. PtN_3-CNT has strong adsorption capacity for the toxic gas molecules, while relatively weaker adsorption performance for the main components of the air except oxygen. The recovery time of each adsorbed molecule calculated at different temperatures showed that, CO_2, H_2O, and N_2 can be desorbed gradually at 298∼498 K, while the toxic gases are always adsorbed stably on the surface of PtN_3-CNT. Considering the excellent thermal stability of PtN_3-CNT at up to 1000 K proved by AIMD, PtN_3-CNT is very suitable to act as an adsorbent to remove toxic gases to achieve the purpose of air purification. Our findings in this report would be beneficial for exploiting possible carbon-based air purification adsorbents with excellent adsorbing ability and good recovery performance.

Keywords: air pollution, gas separation, carbon nanotube, transition metal doping, density functional theory

OPEN ACCESS

Edited by:
Shupeng Zhu,
University of California, Irvine, United States

Reviewed by:
Lei Zhao,
Southwest Petroleum University, China
Haifeng Zheng,
State Key Laboratory of Rare Earth Resources Utilization, Changchun Institute of Applied Chemistry (CAS), China

***Correspondence:**
Wei Liu
weiliu@zafu.edu.cn
Jing Xu
jingxu@zafu.edu.cn

[†] *These authors have contributed equally to this work*

Specialty section:
This article was submitted to Interdisciplinary Climate Studies, a section of the journal Frontiers in Ecology and Evolution

Received: *16 March 2022*
Accepted: *06 April 2022*
Published: *26 April 2022*

Citation:
Yang Y, Liu S, Guo K, Chen L, Xu J and Liu W (2022) Effective Air Purification via Pt-Decorated N_3-CNT Adsorbent. Front. Ecol. Evol. 10:897410. doi: 10.3389/fevo.2022.897410

INTRODUCTION

In recent years, more and more attention has been paid to the impact of air pollution on human health. The effective purification of the air has become a research hotspot in both academia and industry (Zhao and Yang, 2003; Ren et al., 2017). One of the most important ways to purify the air is to adsorb the pollutants through adsorbents (DeCoste and Peterson, 2014; Perreault et al., 2015; Liu et al., 2020). The rapid development of low-dimensional carbon materials provides more options for the detection and separation of atmospheric pollutants (Samaddar et al., 2018; Teng et al., 2018; Cai et al., 2021). Single-walled carbon nanotubes (CNTs) are often used as adsorbents to adsorb certain harmful gases due to their unique tubular structures, huge effective surfaces, high thermal stability and high chemical stability (Li et al., 2018; Poudel and Li, 2018). However, the

pristine CNTs have some disadvantages of few detection gas types, poor recovery performance, low sensitivity, and poor selectivity (Tabtimsai et al., 2020). Therefore, a variety of methods have been proposed to improve the adsorption performance of CNTs, mainly including functional group modification (Guo et al., 2021; Lim et al., 2021), metal doping (Zhou X. et al., 2010; Cui et al., 2018), non-metal doping (Esrafili and Heydari, 2019; Liu et al., 2019), plasma treatment (Babu et al., 2013; Cui et al., 2020; Sun et al., 2021), molecular sieve treatment, and so on (Niimura et al., 2012; Hou et al., 2018).

Noble metals are commonly used catalysts in chemical reactions (Zhang et al., 2021), and they can also serve as active centers for interaction with gas molecules (Tabtimsai et al., 2018). Novel gas sensors have been fabricated and reported by doping metal atoms on the surfaces of transition metal dichaldogenides (Zhang D. et al., 2017; Zhang et al., 2019, 2020). When noble metals are embedded on the surfaces of CNTs, the physical and chemical properties of CNTs will be significantly changed, thus enhancing the adsorption capacity of CNTs to various gas molecules (Zhang et al., 2014). However, the binding of metal atoms with CNTs is often weak and the anchored metal atoms are easy to desorb. Due to the strong coordination interaction between nitrogen atoms and many metal atoms (Wang H. et al., 2021; Wang L. et al., 2021) N_x (x = 3 or 4) groups have been introduced into the surfaces of CNTs to stabilize the adsorption of metal atoms (Feng et al., 2010). The doping of N atoms in CNTs will also introduce novel states near the Fermi level, thus improving the adsorption selectivity and sensitivity of CNTs to gas molecules (Zhou Y. et al., 2010; Gao et al., 2018; Tabtimsai et al., 2020). Hence, the combination of the electron-donating properties of noble metals and electron-attracting properties of N_x groups will result in significant electron localization, which is helpful to promote the stable chemisorption behavior of gas molecules on the surfaces of CNTs (Peng and Cho, 2003; Li et al., 2009).

In this work, the air purification performance of Pt-decorated N_3-CNT as adsorbent was studied using first-principles calculations. The adsorption behaviors and electronic structures of 12 gas molecules on the surface of PtN_3-CNT were investigated. The calculated results confirmed that the N_3 group could effectively enhance the adsorption performance of metal-doped CNTs toward gas molecules through the improvement of electron mobility and chemical activity. The adsorption capacity of PtN_3-CNT to common air pollutants and the main components of the air varies greatly. The recovery time for the gas molecules to desorb from the PtN_3-CNT surface were further calculated at different temperatures.

COMPUTATIONAL METHODS

The Vienna Ab initio Simulation Package (VASP) (Kresse and Furthmüller, 1996) based on density functional theory was used for all the first-principles calculations. The Perdew-Burke-Ernzerhof (PBE) (Perdew et al., 1996) functional in generalized gradient approximation (GGA) (Kohn and Sham, 1965) was used to describe the exchange-correlation interactions. The kinetic energy cutoff was set to 550 eV. The convergence criteria for energy and force in all the calculations were 1×10^{-5} eV and −0.01 eV/Å, respectively. The first Brillouin zone was represented using the Monkhorst-Pack scheme (Chadi, 1977) with a $1 \times 1 \times 2$ K-point mesh. Vacuum layers of 25Å were set in the radial directions of the CNTs to avoid interactions between adjacent structures. The Gaussian smearing method and a denser K-point mesh ($1 \times 1 \times 8$) were used in all the electronic properties calculations. In addition, the van der Waals interaction was considered using DFT-D3 correction method of Grimme et al. (2010). Ab initio molecular dynamics (AIMD) simulations in the canonical ensemble (NVT) with the Nosé-Hoover thermostat (Hoover, 1985) were performed for 5.0 ps with a time-step of 1.0 fs at 1000 K. The stress tensor was calculated every time-step.

To evaluate the adsorption behaviors of gas molecules, we use the adsorption energy (E_{ad}) as the descriptor which is defined as follows:

$$E_{ad} = E_{PtN_3-CNT/gas} - E_{PtN_3-CNT} - E_{gas} \quad (1)$$

where $E_{PtN_3-CNT/gas}$, E_{PtN_3-CNT}, E_{gas} represent the total energy of the adsorption system, PtN_3-CNT and isolated gas molecules, respectively. In addition, the bader charge (Bader and Beddall, 1972) is used to analyze the charge transfer between the gas molecules and the modified surface. The charge transfer can be defined as the number of electrons carried by the gas molecules after adsorption, because the electron value carried by the molecule is always zero before adsorption. Positive values indicate charge transfer from PtN_3-CNT to gas molecules, while negative values indicate the reverse charge transfer path.

RESULTS

Geometric and Electronic Structures of PtN_3-CNT

Zigzag (8,0) single-walled carbon nanotube was chosen as the substrate to construct the PtN_3-CNT structure by firstly deleting one carbon atom to form a single-vacancy defect, secondly substitutional doping of three carbon atoms possessing dangling bonds with nitrogen atoms, and finally adsorbing one Pt atom at the center of the N_3 group. The geometric and electronic structures of PtN_3-CNT were investigated. **Figure 1A** shows the top and side views of the geometric configuration of the optimized PtN_3-CNT. The Pt atom is captured by the N_3 group, and the lengths of Pt-N bonds are 1.96 and 2.08Å, respectively. The binding energies (E_b) for one Pt atom on the surface of CNTs were calculated using the following formula:

$$E_b = E_{PtN_3-CNT} - E_{N_3-CNT} - E_{Pt} \quad (2)$$

where E_{PtN_3-CNT}, E_{N_3-CNT}, E_{Pt} represent the energies of PtN_3-CNT, pure N_3-CNT and Pt atom, respectively. The obtained negative E_b (−3.20 eV) value demonstrates that the binding of Pt atom on the surface of CNT *via* N_3 groups is thermodynamically preferable. Furthermore, to investigate the thermal stability of PtN_3-CNT, ab initio molecular dynamics (AIMD) simulations

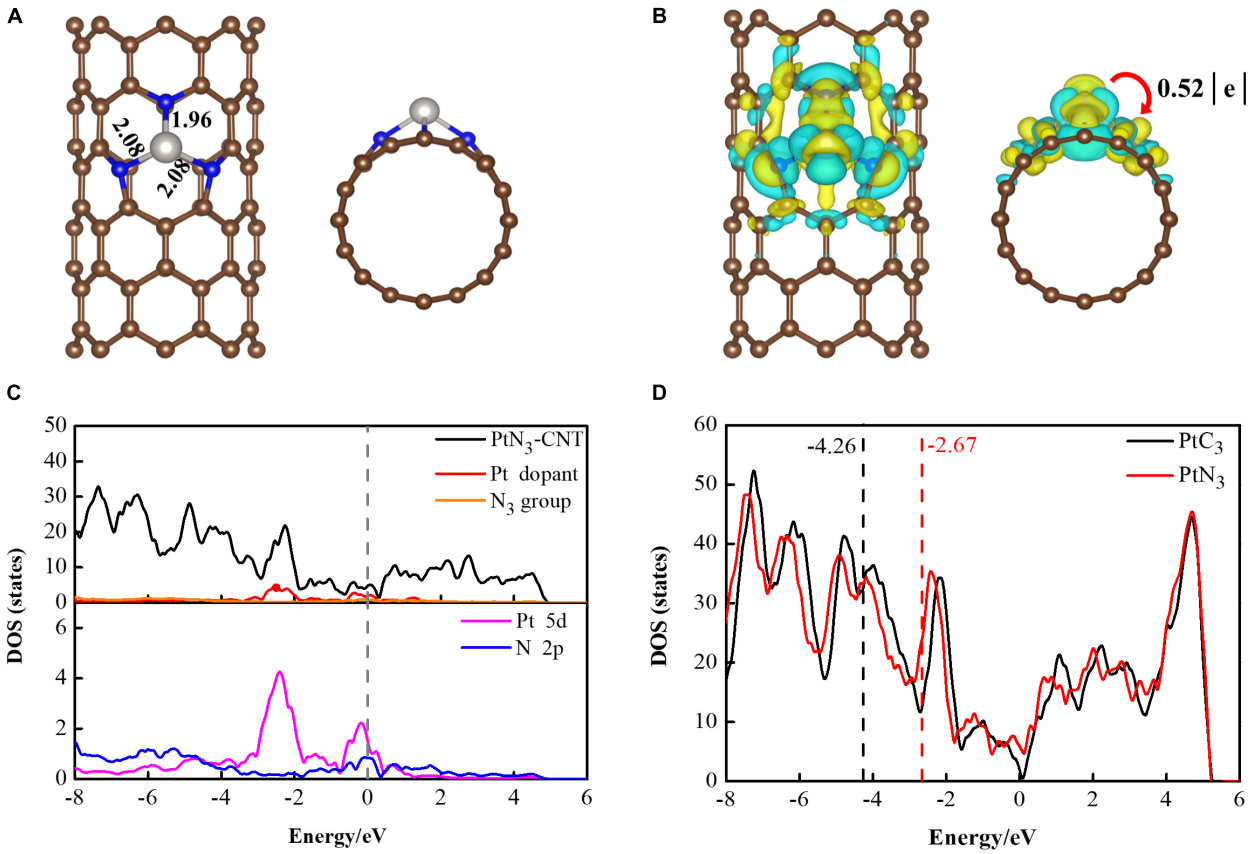

FIGURE 1 | (A) The top and side views of the optimized geometries of PtN_3-CNT; **(B)** Deformation charge distribution of PtN_3-CNT. The yellow area and cyan area represent the accumulation and consumption of electrons, respectively. The value of the isosurface level is 0.0011 e/Å^3. **(C)** DOS and PDOS of PtN_3-CNT; **(D)** *d*-band centers of PtN_3-CNT and PtC_3-CNT. Brown, blue, gray balls represent C, N, and Pt atoms, respectively.

were performed at 1000 K. The obtained results were shown in **Supplementary Figure 1**. No reconstruction of the PtN_3-CNT structure was found, implying that PtN_3-CNT can withstand temperatures up to 1000 K.

The result of deformation charge distribution (DCD) of PtN_3-CNT are shown in **Figure 1B**, which indicates that the N_3 group could act as the electron active center to withdraw electrons from the carbon nanotube and Pt atom. The Pt atom acts as an electron donor to release 0.52 *e* to N_3-CNT, and the three N atoms obtain 0.14 *e*, 0.13 *e* and 0.12 *e*, respectively. This is because the lone pair electrons and non-bonded electrons carried on the sp^2 orbitals of the three N atoms produce highly localized acceptor-like states at the Fermi level (Rangel and Sansores, 2014), and the strong electron withdrawing properties of the N_3 center further enhance the electron distribution.

Next, the density of states (DOS) and the projected density of states (PDOS) of PtN_3-CNT and PtC_3-CNT were calculated to further understand the electronic behaviors and the effect of the N_3 group. As shown in **Figure 1C**, the partial DOS curve of the metal dopant and the N_3 group are in good agreement with the total DOS curve of PtN_3-CNT, especially in the region close to the Fermi level. In the PtN_3-CNT system, it can be seen that due to the doping of N atoms in carbon nanotubes, the electron-donating properties of Pt are combined with the electron-absorbing properties of N_3 group, leading to significant electron localization, thus forming a new state near the Fermi level, which will improve the adsorption selectivity and sensitivity of carbon nanotubes to gas molecules. The contribution of the Pt dopant to the total DOS in PtN_3-CNT is greater than that in PtC_3-CNT (shown in **Supplementary Figure 2**), which endows the doped Pt atom a greater regulatory effect on the electronic behavior of PtN_3-CNT. From the PDOS, it is shown that there exists a large-area overlap between the Pt 5*d* orbital and the N 2*p* orbital. This means that the Pt atom chemically interacts with N_3-CNT, leading to significant electron transfer and making PtN_3-CNT more active (Zhao and Wu, 2018).

We also calculated the *d*-band center structures and positions of PtN_3-CNT and PtC_3-CNT to evaluate whether the N_3 group has enhanced the gas adsorption ability of Pt-decorated CNT (shown in **Figure 1D**). The result illustrates that the *d*-band center value of the PtC_3-CNT system is −4.26 eV, while the value of the PtN_3-CNT system is −2.67 eV, which is closer to the Fermi level than the PtC_3-CNT system. As the position of the *d*-band center increases, the anti-bonding orbital formed by the system to adsorb gas molecules will be pushed up. The higher the anti-bonding orbital position is, the more stable the

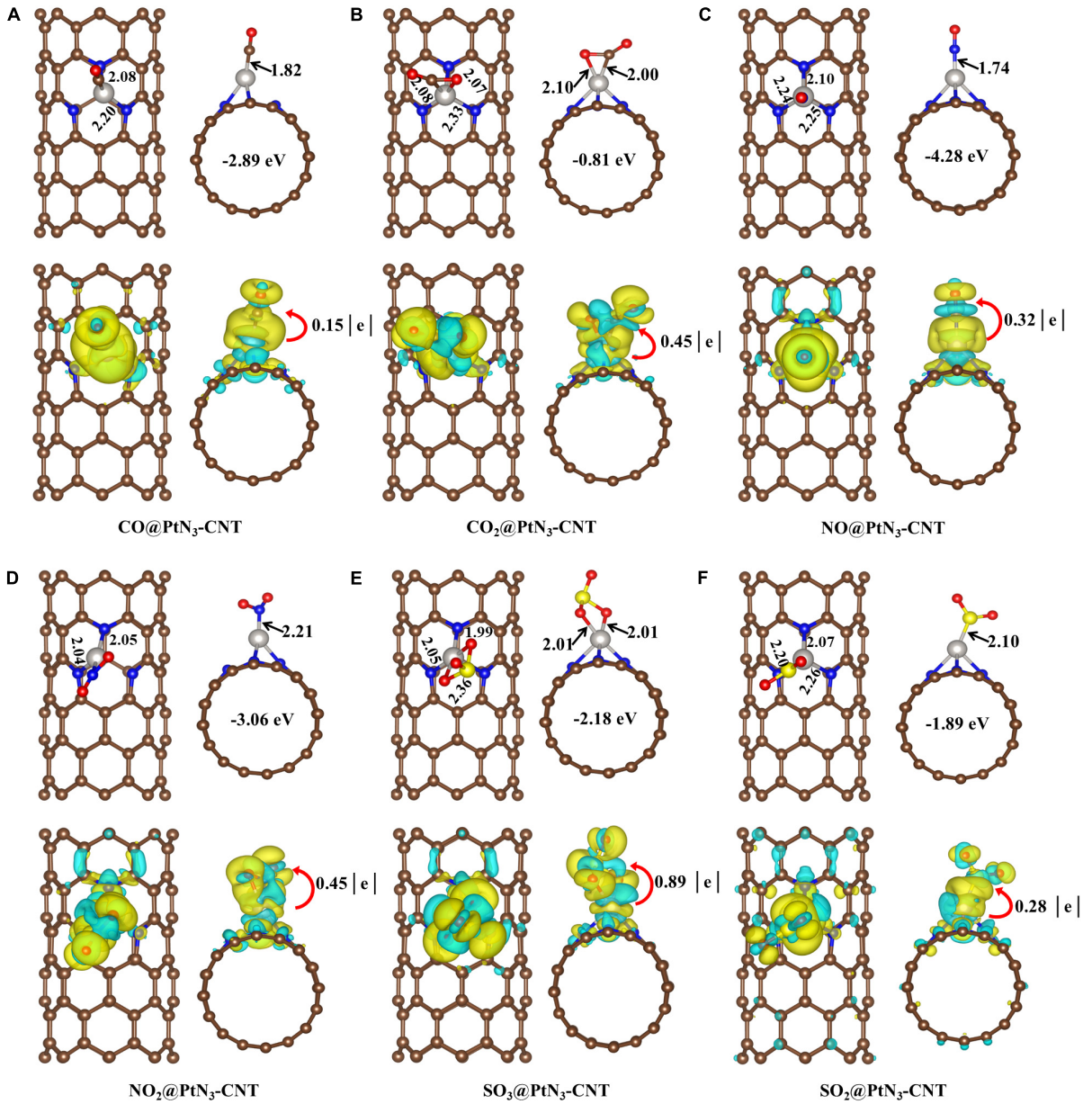

FIGURE 2 | Adsorption structures and deformation charge distribution of **(A)** CO@PtN_3-CNT system; **(B)** CO_2@PtN_3-CNT system; **(C)** NO@PtN_3-CNT system; **(D)** NO_2@PtN_3-CNT system; **(E)** SO_3@PtN_3-CNT system; and **(F)** SO_2@PtN_3-CNT system. In the middle of the side views are the adsorption energies of the gas molecules. Yellow and red balls represent S and O atoms, respectively. The yellow area and cyan area represent the accumulation and consumption of electrons, respectively.

system is after adsorbing gas molecules. Therefore, the PtN_3-CNT system is more favorable for gas adsorption than the PtC_3-CNT system, and the adsorption ability of Pt-decorated CNT toward gas molecules is effectively enhanced.

Adsorption of Gas Molecules on the Surface of PtN_3-CNT

The adsorption of 12 kinds of gas molecules on the surface of PtN_3-CNT were investigated, including the main components of the air (N_2, O_2, H_2O, and CO_2), the most common air pollutants nitrous oxides (NO, NO_2), sulfur oxides (SO_2, SO_3), CO, O_3, NH_3, and H_2S. For each adsorbed gas molecule, a variety of different adsorption structures were obtained and only the most stable geometric structures are discussed in the following sections. These 12 gas molecules are divided into three categories for discussion, namely the oxides, the hydrides and the elemental gases.

The optimized structures for the oxides adsorption on PtN_3-CNT and the DCD figures are shown in **Figure 2**. CO, NO, NO_2,

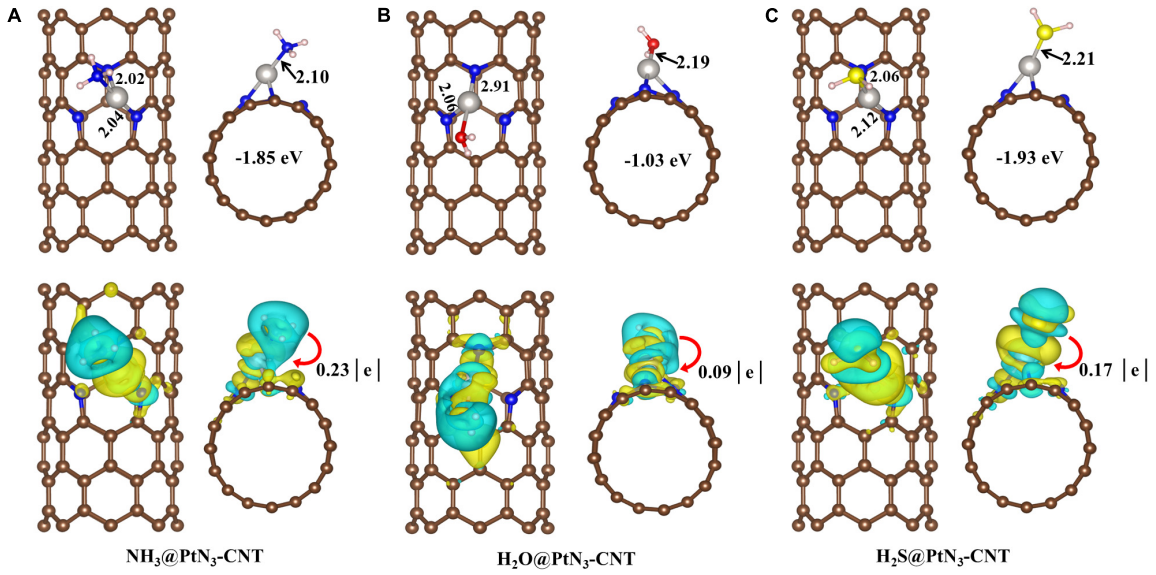

FIGURE 3 | Adsorption structures and deformation charge distribution of **(A)** NH_3@PtN_3-CNT system; **(B)** H_2O@PtN_3-CNT system; **(C)** H_2S@PtN_3-CNT system. Light pink ball represents H atom. The yellow area and cyan area represent the accumulation and consumption of electrons, respectively.

and SO_2 molecules interact with the dopant Pt atoms through a single atom forming new Pt-C (1.82Å), Pt-N (1.74Å for NO, and 2.21Å for NO_2), and Pt-S (2.10Å) bonds while CO_2 and SO_3 are adsorbed on the surface by forming two bonds. The newly formed Pt-C, Pt-N, and Pt-S bonds in the adsorption structures of CO, NO, and SO_2 are shorter than the sum of the covalent bond radius of Pt and C (1.98Å), Pt and N (1.94Å), Pt and S (2.26Å), indicating that the noble metal dopant (Pt) has a strong binding force to CO, NO, and SO_2 molecules, resulting in the chemisorption properties of these systems. The adsorption energies of these oxides vary in the range of −0.81∼−4.28 eV, and 0.15∼0.89 electrons are transferred from the adsorbent surfaces to the gas molecules. Among these oxides, the adsorption of CO_2 on the surface of PtN_3-CNT is the weakest.

As shown in **Figure 3**, the three hydrides (NH_3, H_2O, and H_2S) are adsorbed stably on PtN_3-CNT with adsorption energies of −1.85, −1.03, and −1.93 eV, respectively. The adsorption of H_2O has the smallest adsorption energy in the considered hydrides. In the adsorption structures, Pt atoms coordinate with the N, O, and S atoms as in the adsorption of oxides, and the newly formed Pt-N, Pt-O, and Pt-S bonds are 2.10, 2.19, and 2.21Å, respectively. Moreover, unlike the adsorption of oxides, 0.23, 0.09, and 0.17 e are transferred from the gas molecules to the adsorbent PtN_3-CNT, which is because that the electronegativity of hydrogen atoms is much weaker.

The adsorption structures of the three elemental gases (O_3, O_2, N_2) on PtN_3-CNT are shown in **Figure 4**. The adsorption energies of O_3 and O_2 (−3.59 and −3.24 eV, respectively) on PtN_3-CNT are much larger than that of N_2 (−1.36 eV), which may be due to the fact that two oxygen atoms are coordinated with the dopant Pt in the adsorption structures of O_3 and O_2. The newly formed Pt-O bonds in O_3@PtN_3-CNT and O_2@PtN_3-CNT are 1.99, 1.95, and 2.07Å, respectively. The newly formed Pt-N bond in N_2@PtN_3-CNT (1.89Å) is smaller than the sum of the covalent bond radius of Pt and N (1.94Å), indicating that the adsorption of N_2 molecules on the surface of PtN_3-CNT is chemical adsorption. 0.70, 0.59, and 0.22 e are transferred from the elemental gas molecules to the adsorbent surfaces, respectively.

In all the adsorption structures discussed above, the chemical Pt-N bonds in PtN_3-CNT are stretched by 0.01–0.29Å after adsorption, and one Pt-N is even broken in some adsorption structures (CO, NO_2, NH_3, H_2O, H_2S, O_2, and N_2). After adsorption, the chemical bonds in the gas molecules are all elongated relative to free molecules, indicating that these gas molecules are activated after adsorption on the PtN_3-CNT surfaces. Moreover, the adsorption energies of some gas molecules on Pt-CNT (−1.73 eV for CO, −3.53 eV for NO, −1.37 eV for NH_3, −1.06 eV for N_2, respectively) have been reported previously. These E_{ad} are 0.30∼1.16 eV smaller than the corresponding adsorption energies on PtN_3-CNT, confirming that the N_3 dopant have effectively improved the reactivity of CNTs, thereby enhancing the adsorption performance of the system for gas molecules.

Next, the electronic structures of gas@PtN_3-CNT systems are investigated. From the above discussion, it can be found that the gas molecules are adsorbed on the surface of PtN_3-CNT through the coordination of Pt with C, N, O, and S atoms, respectively. The DOS and PDOS of the gas molecules with the largest E_{ad} (CO, NO, O_3, and H_2S) in each coordination mode are shown in **Figure 5**, and those of the other gases are shown in **Supplementary Figure 3**. Generally, the total DOS curves of gas@PtN_3-CNT are very similar with that of isolated PtN_3-CNT, except that the total DOS curves of the adsorbed systems shift to the high energy region. This could be attributed to the electron-withdrawing behavior of PtN_3-CNT that results

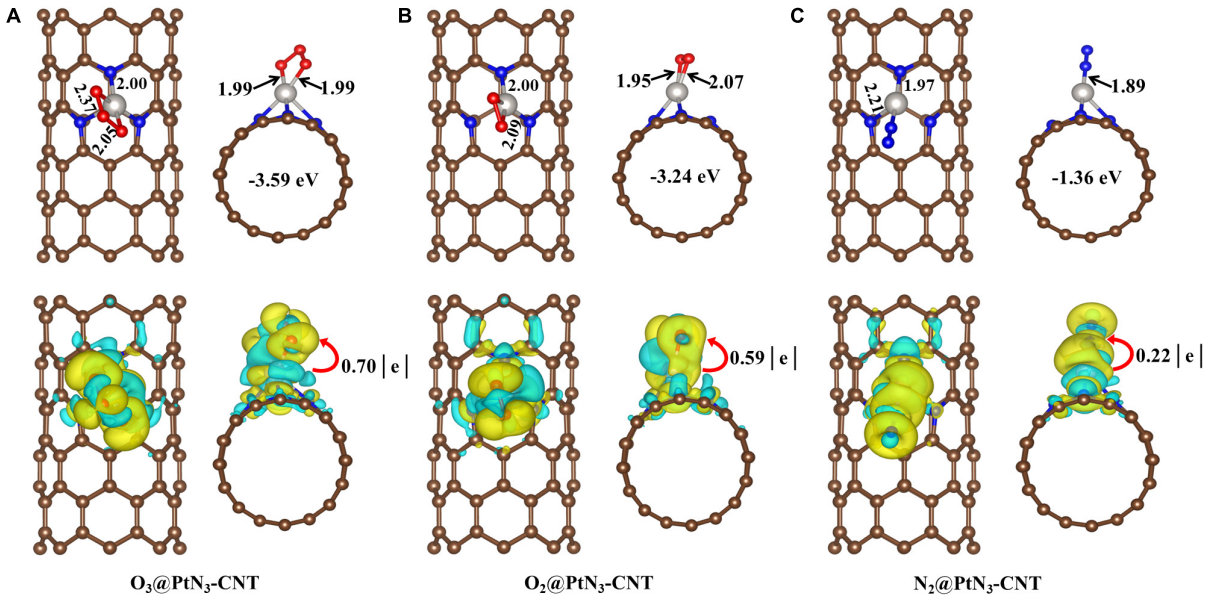

FIGURE 4 | Adsorption structures and deformation charge distribution of **(A)** O_3@PtN_3-CNT system; **(B)** O_2@PtN_3-CNT system; **(C)** N_2@PtN_3-CNT system. The yellow area and cyan area represent the accumulation and consumption of electrons, respectively.

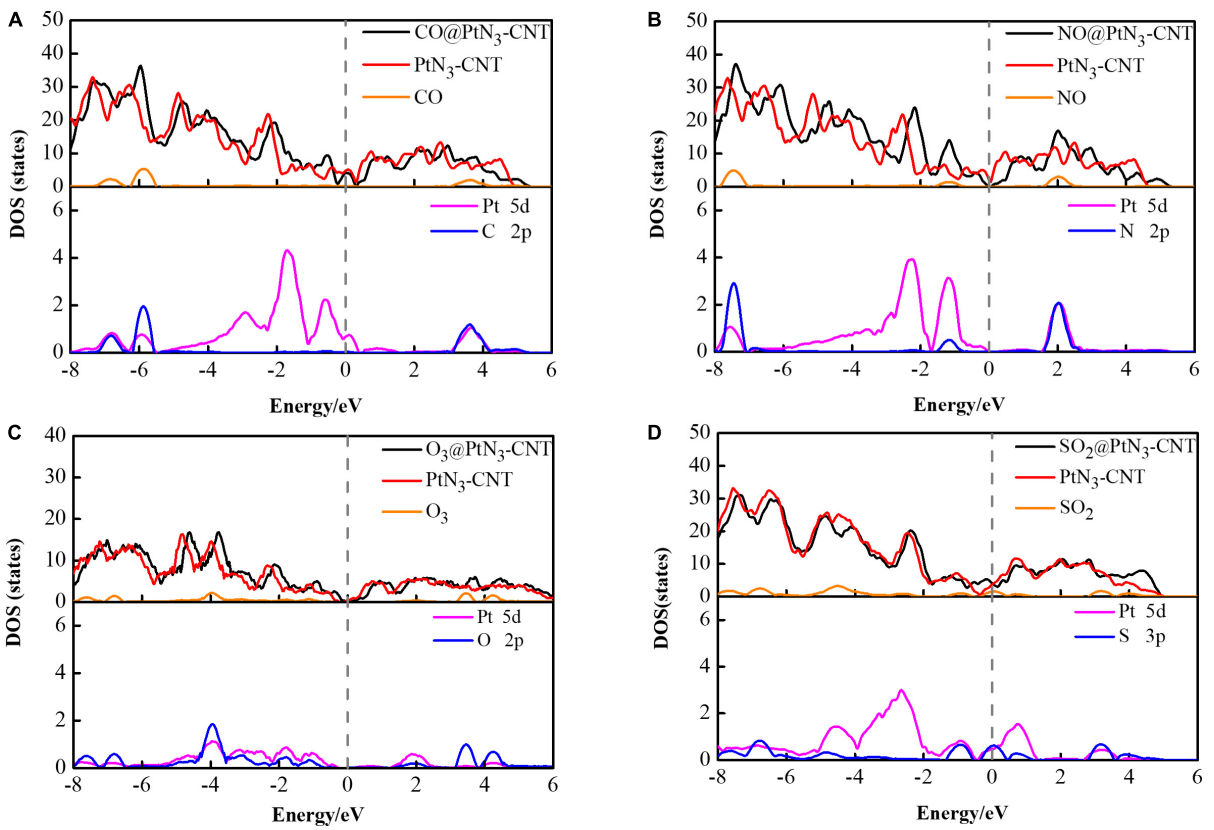

FIGURE 5 | DOS and PDOS of **(A)** CO@PtN_3-CNT system; **(B)** NO@PtN_3-CNT system; **(C)** O_3@PtN_3-CNT system; and **(D)** H_2S@PtN_3-CNT system. The dashed line represents the Fermi level.

TABLE 1 | Adsorption energies (E_{ad}), distances between Pt and the coordinated atoms (D), and the charge transferred between PtN_3-CNT and the gas molecules for Gas@PtN_3-CNT systems (Q_T).

Gas	E_{ad} (eV)	D (Å)	Q_T (e)	Gas	E_{ad} (eV)	D (Å)	Q_T (e)
CO	−2.89	1.82	0.15	NH_3	−1.85	2.10	−0.23
CO_2	−0.81	2.00 2.10	0.45	H_2S	−1.93	2.21	−0.17
NO	−4.28	1.74	0.32	H_2O	−1.03	2.19	−0.09
NO_2	−3.06	2.21	0.45	O_3	−3.59	1.99	0.70
SO_3	−2.18	2.01	0.89	O_2	−3.24	1.95 2.07	0.59
SO_2	−1.89	2.10	0.28	N_2	−1.36	1.89	0.22

in an increase of the effective Coulomb potential (Zhang et al., 2018). The adsorbed gas molecules contribute dramatically to the total DOS in some specific areas (for CO, near 3.75, −5.82, and −6.85 eV; for NO, near 2.01, −1.15, and −7.42 eV; for O_3, near 4.25, 3.45, −4.15, −6.75, and −7.71 eV; for H_2S, near 2.85 and −7.68 eV), which are derived from the outermost *p* orbitals of the coordinated atoms in the gas molecules. And obvious deformations have taken place at these areas in the total DOS curves. Meanwhile, there exist apparent overlaps between the Pt *5d* and the outmost *p* orbitals of the coordination atoms, indicating the obvious chemical interactions between PtN_3-CNT and the adsorbed gas molecules. It can also be concluded that these outermost *p* orbitals of the coordinated atoms in the adsorbed gas molecules play an important role in the adsorption of gases on PtN_3-CNT.

Application of PtN_3-CNT in Air Purification

Previous calculated results show that PtN_3-CNT has strong adsorption capacity for the toxic gas molecules (NO, NO_2, SO_3, SO_2, CO, NH_3, H_2S, and O_3) with E_{ad} in the range of −1.85∼−4.28 eV, while relatively weaker adsorption performance for the main components of the air except oxygen (N_2, H_2O, and CO_2) with E_{ad} in the range of −0.81∼−1.36 eV. If these gas molecules were adsorbed on the surface of PtN_3-CNT, it would be very difficult for the toxic gas molecules to desorb, but the main components of the air may be desorbed by heating. Therefore, we assume that PtN_3-CNT possess the potential as an excellent gas adsorbent for the air purification.

To prove this hypothesis, the recovery time for the gas molecules to desorb from the PtN_3-CNT surface was investigated based on the transition state theory and van't Hoff-Arrhenius expression (Zhang et al., 2009) as below:

$$\tau = A^{-1} e^{(-E_a / K_B T)} \quad (3)$$

where A, K_B, and T represent the attempt frequency (10^{12} s^{-1}) (Peng et al., 2004), the Boltzmann constant [8.318×10^{-3} kJ (mol K)$^{-1}$] and the temperature, respectively. E_a is the desorption potential barrier and can be considered the same as E_{ad}. From Equation (3), it can be concluded that the recovery time increases exponentially with the increase of E_{ad}. The larger the E_{ad} is, the more difficult the gas desorption process is. And increasing the temperature can effectively accelerate this process (Schedin et al., 2007; Yang et al., 2017; Zhang X. et al., 2017). According to the previously obtained E_{ad} as shown in **Table 1**,

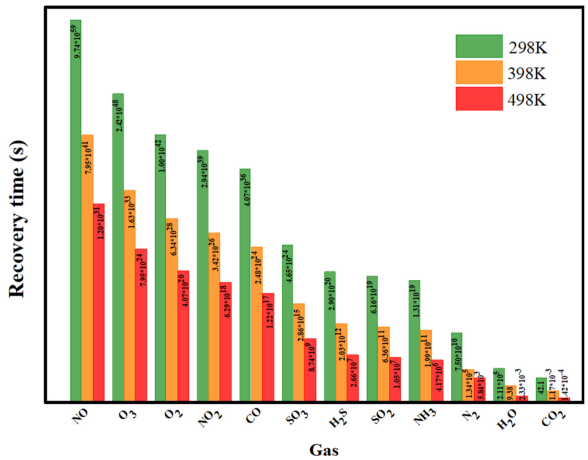

FIGURE 6 | Recovery time for the Gas@PtN_3-CNT systems at various temperatures.

the recovery time for the desorption of all the gas molecules from the PtN_3-CNT surface at 298, 398, 498 K were calculated (listed in **Supplementary Table 1**) and plotted in **Figure 6**. The results showed that the desorption of all the gas molecules is very unrealistic at room temperature, except for CO_2 which requires only 42.10 s to desorb from the surface of PtN_3-CNT. The good adsorption performance and short recovery time at ambient temperature make PtN_3-CNT an excellent candidate for CO_2 sensing. When the temperature is increased by 100–398 K, H_2O can be desorbed with a recovery time of 9.38 s. When the temperature is increased again by 100–498 K, N_2 will be desorbed with a recovery time of 1.62 h, while all the toxic gas molecules and O_2 are still adsorbed stably on the surface of PtN_3-CNT. Therefore, considering the excellent thermal stability of PtN_3-CNT at up to 1000 K proved by AIMD previously, and the adsorption and desorption behavior at different temperature, PtN_3-CNT structure is very suitable to act as an adsorbent to remove toxic gases to achieve the purpose of air purification.

CONCLUSION

In summary, we proposed that PtN_3-CNT is an excellent adsorbent for air purification in this work. The adsorption of four main components of the air (N_2, O_2, H_2O, CO_2) and eight common air pollutants (NO, NO_2, SO_3, SO_2, CO,

O_3, NH_3, H_2S) on the surface of PtN_3-CNT were studied using first-principles calculations. The calculation results about *d*-band centers and adsorption energies confirmed that the N_3 dopant have effectively improved the reactivity of CNTs, thereby enhancing the adsorption performance of PtN_3-CNT for gas molecules. All the considered gases can be adsorbed stably on PtN_3-CNT, and the adsorption energies for the toxic gas molecules (−1.85∼−4.28 eV) are larger than those for the main components of the air except oxygen (−0.81∼−1.36 eV). The recovery time for the desorption of all the gas molecules from the PtN_3-CNT surface at 298, 398, 498 K were calculated. The obtained results showed that CO_2, H_2O, and N_2 can be desorbed at 298, 398, and 498 K, respectively, while all the air pollutants and O_2 are always adsorbed stably. Therefore, PtN_3-CNT can be used to purify the air by firstly adsorbing the gas mixture and then gradually releasing the air by heating.

DATA AVAILABILITY STATEMENT

The raw data supporting the conclusions of this article will be made available by the authors, without undue reservation.

AUTHOR CONTRIBUTIONS

WL, JX, YY, and SL conceived the research. YY, KG, and SL performed the calculations and analyzed the data. WL, JX, and YY wrote the manuscript. LC helped to revise the manuscript. All authors discussed and commented on the manuscript and approved the submitted version.

FUNDING

This work was supported by the Zhejiang Provincial Natural Science Foundation of China (No. LQ20B030002) and the National Natural Science Foundation of China (Nos. 12075211, 11975206, 11875236, and U1832150).

SUPPLEMENTARY MATERIAL

The Supplementary Material for this article can be found online at: https://www.frontiersin.org/articles/10.3389/fevo.2022.897410/full#supplementary-material

REFERENCES

Babu, D. J., Lange, M., Cherkashinin, G., Issanin, A., Staudt, R., and Schneider, J. J. (2013). Gas adsorption studies of CO_2 and N_2 in spatially aligned double-walled carbon nanotube arrays. *Carbon* 61, 616–623. doi: 10.1016/j.carbon.2013.05.045

Bader, R. F. W., and Beddall, P. M. (1972). Virial field relationship for molecular charge distributions and the spatial partitioning of molecular properties. *J. Chem. Phys.* 56, 3320–3329. doi: 10.1063/1.1677699

Cai, G., Yan, P., Zhang, L., Zhou, H.-C., and Jiang, H.-L. (2021). Metal–Organic framework-based hierarchically porous materials: synthesis and applications. *Chem. Rev.* 121, 12278–12326. doi: 10.1021/acs.chemrev.1c00243

Chadi, D. J. (1977). Special points for brillouin-zone integrations. *Phys. Rev. B* 16, 1746–1747. doi: 10.1103/PhysRevB.16.1746

Cui, H., Zhang, X., Chen, D., and Tang, J. (2018). Adsorption mechanism of SF_6 decomposed species on pyridine-like PtN_3 embedded CNT: a DFT study. *Appl. Surf. Sci.* 447, 594–598. doi: 10.1016/j.apsusc.2018.03.232

Cui, J., Zhang, K., Zhang, X., and Lee, Y. (2020). A computational study to design zeolite-templated carbon materials with high performance for CO_2/N_2 separation. *Microporous Mesoporous Mater.* 295:109947. doi: 10.1016/j.micromeso.2019.109947

DeCoste, J. B., and Peterson, G. W. (2014). Metal–Organic frameworks for air purification of toxic chemicals. *Chem. Rev.* 114, 5695–5727. doi: 10.1021/cr4006473

Esrafili, M. D., and Heydari, S. (2019). B-doped C_3N monolayer: a robust catalyst for oxidation of carbon monoxide. *Theor. Chem. Acc.* 138:57. doi: 10.1007/s00214-019-2444-z

Feng, H., Ma, J., and Hu, Z. (2010). Nitrogen-doped carbon nanotubes functionalized by transition metal atoms: a density functional study. *J. Mater. Chem.* 20:1702. doi: 10.1039/b915667d

Gao, Z., Sun, Y., Li, M., Yang, W., and Ding, X. (2018). Adsorption sensitivity of Fe decorated different graphene supports toward toxic gas molecules (CO and NO). *Appl. Surf. Sci.* 456, 351–359. doi: 10.1016/j.apsusc.2018.06.112

Grimme, S., Antony, J., Ehrlich, S., and Krieg, H. (2010). A consistent and accurate ab initio parametrization of density functional dispersion correction (DFT-D) for the 94 elements H-Pu. *J. Chem. Phys.* 132:154104. doi: 10.1063/1.3382344

Guo, K., Liu, S., Tu, H., Wang, Z., Chen, L., Lin, H., et al. (2021). Crown ethers in hydrogenated graphene. *Phys. Chem. Chem. Phys.* 23, 18983–18989. doi: 10.1039/D1CP03069H

Hoover, W. G. (1985). Canonical dynamics: equilibrium phase-space distributions. *Phys. Rev. A* 31, 1695–1697. doi: 10.1103/PhysRevA.31.1695

Hou, J., Zhang, H., Hu, Y., Li, X., Chen, X., Kim, S., et al. (2018). Carbon nanotube networks as nanoscaffolds for fabricating ultrathin carbon molecular sieve membranes. *ACS Appl. Mater. Interfaces* 10, 20182–20188. doi: 10.1021/acsami.8b04481

Kohn, W., and Sham, L. J. (1965). Self-Consistent equations including exchange and correlation effects. *Phys. Rev.* 140, A1133–A1138. doi: 10.1103/PhysRev.140.A1133

Kresse, G., and Furthmüller, J. (1996). Efficiency of ab-initio total energy calculations for metals and semiconductors using a plane-wave basis set. *Comput. Mater. Sci.* 6, 15–50. doi: 10.1016/0927-0256(96)00008-0

Li, Y., Chen, J., Cai, P., and Wen, Z. (2018). An electrochemically neutralized energy-assisted low-cost acid-alkaline electrolyzer for energy-saving electrolysis hydrogen generation. *J. Mater. Chem. A* 6, 4948–4954. doi: 10.1039/C7TA10374C

Li, Y.-H., Hung, T.-H., and Chen, C.-W. (2009). A first-principles study of nitrogen- and boron-assisted platinum adsorption on carbon nanotubes. *Carbon* 47, 850–855. doi: 10.1016/j.carbon.2008.11.048

Lim, N., Kim, K. H., and Byun, Y. T. (2021). Preparation of defected SWCNTs decorated with en-APTAS for application in high-performance nitric oxide gas detection. *Nanoscale* 13, 6538–6544. doi: 10.1039/D0NR08919B

Liu, D., Li, C., Wu, J., and Liu, Y. (2020). Novel carbon-based sorbents for elemental mercury removal from gas streams: a review. *Chem. Eng. J.* 391:123514. doi: 10.1016/j.cej.2019.123514

Liu, P., Liang, J., Xue, R., Du, Q., and Jiang, M. (2019). Ruthenium decorated boron-doped carbon nanotube for hydrogen storage: a first-principle study. *Int. J. Hydrog. Energy* 44, 27853–27861. doi: 10.1016/j.ijhydene.2019.09.019

Niimura, S., Fujimori, T., Minami, D., Hattori, Y., Abrams, L., Corbin, D., et al. (2012). Dynamic quantum molecular sieving separation of D_2 from H_2 –D_2 mixture with nanoporous materials. *J. Am. Chem. Soc.* 134, 18483–18486. doi: 10.1021/ja305809u

Peng, S., and Cho, K. (2003). Ab initio study of doped carbon nanotube sensors. *Nano Lett.* 3, 513–517. doi: 10.1021/nl034064u

Peng, S., Cho, K., Qi, P., and Dai, H. (2004). Ab initio study of CNT NO2 gas sensor. *Chem. Phys. Lett.* 387, 271–276. doi: 10.1016/j.cplett.2004.02.026

Perdew, J. P., Burke, K., and Ernzerhof, M. (1996). Generalized gradient approximation made simple. *Phys. Rev. Lett.* 77, 3865–3868. doi: 10.1103/PhysRevLett.77.3865

Perreault, F., Fonseca de Faria, A., and Elimelech, M. (2015). Environmental applications of graphene-based nanomaterials. *Chem. Soc. Rev.* 44, 5861–5896. doi: 10.1039/C5CS00021A

Poudel, Y. R., and Li, W. (2018). Synthesis, properties, and applications of carbon nanotubes filled with foreign materials: A review. *Mater. Today Phys.* 7, 7–34. doi: 10.1016/j.mtphys.2018.10.002

Rangel, E., and Sansores, E. (2014). Theoretical study of hydrogen adsorption on nitrogen doped graphene decorated with palladium clusters. *Int. J. Hydrog. Energy* 39, 6558–6566. doi: 10.1016/j.ijhydene.2014.02.062

Ren, H., Koshy, P., Chen, W.-F., Qi, S., and Sorrell, C. C. (2017). Photocatalytic materials and technologies for air purification. *J. Hazard. Mater.* 325, 340–366. doi: 10.1016/j.jhazmat.2016.08.072

Samaddar, P., Son, Y.-S., Tsang, D. C. W., Kim, K.-H., and Kumar, S. (2018). Progress in graphene-based materials as superior media for sensing, sorption, and separation of gaseous pollutants. *Coord. Chem. Rev.* 368, 93–114. doi: 10.1016/j.ccr.2018.04.013

Schedin, F., Geim, A. K., Morozov, S. V., Hill, E. W., Blake, P., Katsnelson, M. I., et al. (2007). Detection of individual gas molecules adsorbed on graphene. *Nat. Mater.* 6, 652–655. doi: 10.1038/nmat1967

Sun, X., Bao, J., Li, K., Argyle, M. D., Tan, G., Adidharma, H., et al. (2021). Advance in using plasma technology for modification or fabrication of carbon-based materials and their applications in environmental, material, and energy fields. *Adv. Funct. Mater.* 31:2006287. doi: 10.1002/adfm.202006287

Tabtimsai, C., Rakrai, W., Phalinyot, S., and Wanno, B. (2020). Interaction investigation of single and multiple carbon monoxide molecules with Fe-, Ru-, and Os-doped single-walled carbon nanotubes by DFT study: applications to gas adsorption and detection nanomaterials. *J. Mol. Model.* 26:186. doi: 10.1007/s00894-020-04457-7

Tabtimsai, C., Somtua, T., Motongsri, T., and Wanno, B. (2018). A DFT study of H_2CO and HCN adsorptions on 3d, 4d, and 5d transition metal-doped graphene nanosheets. *Struct. Chem.* 29, 147–157. doi: 10.1007/s11224-017-1013-0

Teng, W., Bai, N., Chen, Z., Shi, J., Fan, J., and Zhang, W. (2018). Hierarchically porous carbon derived from metal-organic frameworks for separation of aromatic pollutants. *Chem. Eng. J.* 346, 388–396. doi: 10.1016/j.cej.2018.04.051

Wang, H., Li, J., Li, K., Lin, Y., Chen, J., Gao, L., et al. (2021). Transition metal nitrides for electrochemical energy applications. *Chem. Soc. Rev.* 50, 1354–1390. doi: 10.1039/D0CS00415D

Wang, L., Zhu, C., Xu, M., Zhao, C., Gu, J., Cao, L., et al. (2021). Boosting activity and stability of metal single-atom catalysts via regulation of coordination number and local composition. *J. Am. Chem. Soc.* 143, 18854–18858. doi: 10.1021/jacs.1c09498

Yang, A.-J., Wang, D.-W., Wang, X.-H., Chu, J.-F., Lv, P.-L., Liu, Y., et al. (2017). Phosphorene: a promising candidate for highly sensitive and selective sf6 decomposition gas sensors. *IEEE Electron Device Lett.* 38, 963–966. doi: 10.1109/LED.2017.2701642

Zhang, A., Liang, Y., Zhang, H., Geng, Z., and Zeng, J. (2021). Doping regulation in transition metal compounds for electrocatalysis. *Chem. Soc. Rev.* 50, 9817–9844. doi: 10.1039/D1CS00330E

Zhang, D., Cao, Y., Yang, Z., and Wu, J. (2020). Nanoheterostructure construction and DFT study of Ni-Doped In_2O_3 Nanocubes/WS_2 hexagon nanosheets for formaldehyde sensing at room temperature. *ACS Appl. Mater. Interfaces* 12, 11979–11989. doi: 10.1021/acsami.9b15200

Zhang, D., Wu, J., Li, P., and Cao, Y. (2017). Room-temperature SO_2 gas sensing properties based on metaldoped MoS_2 nanoflower: an experimental and density functional theory Investigation. *J. Mater. Chem. A* 5, 20666–20677. doi: 10.1039/C7TA07001B

Zhang, D., Yang, Z., Li, P., Pang, M., and Xue, Q. (2019). Flexible self-powered high-performance ammonia sensor based on Au-decorated MoSe2 nanoflowers driven by single layer MoS_2-flake piezoelectric nanogenerator. *Nano Energy* 65:103974. doi: 10.1016/j.nanoen.2019.103974

Zhang, X., Cui, H., Chen, D., Dong, X., and Tang, J. (2018). Electronic structure and H_2S adsorption property of Pt_3 cluster decorated (8, 0) SWCNT. *Appl. Surf. Sci.* 428, 82–88. doi: 10.1016/j.apsusc.2017.09.084

Zhang, X., Dai, Z., Chen, Q., and Tang, J. (2014). A DFT study of SO_2 and H_2S gas adsorption on Au-doped single-walled carbon nanotubes. *Phys. Scr.* 89:065803. doi: 10.1088/0031-8949/89/6/065803

Zhang, X., Gao, B., Creamer, A. E., Cao, C., and Li, Y. (2017). Adsorption of VOCs onto engineered carbon materials: a review. *J. Hazard. Mater.* 338, 102–123. doi: 10.1016/j.jhazmat.2017.05.013

Zhang, Y.-H., Chen, Y.-B., Zhou, K.-G., Liu, C.-H., Zeng, J., Zhang, H.-L., et al. (2009). Improving gas sensing properties of graphene by introducing dopants and defects: a first-principles study. *Nanotechnology* 20:185504. doi: 10.1088/0957-4484/20/18/185504

Zhao, C., and Wu, H. (2018). A first-principles study on the interaction of biogas with noble metal (Rh, Pt, Pd) decorated nitrogen doped graphene as a gas sensor: a DFT study. *Appl. Surf. Sci.* 435, 1199–1212. doi: 10.1016/j.apsusc.2017.11.146

Zhao, J., and Yang, X. (2003). Photocatalytic oxidation for indoor air purification: a literature review. *Build. Environ.* 38, 645–654. doi: 10.1016/S0360-1323(02)00212-3

Zhou, X., Tian, W. Q., and Wang, X.-L. (2010). Adsorption sensitivity of Pd-doped SWCNTs to small gas molecules. *Sens. Actuators B: Chem.* 151, 56–64. doi: 10.1016/j.snb.2010.09.054

Zhou, Y., Neyerlin, K., Olson, T. S., Pylypenko, S., Bult, J., Dinh, H. N., et al. (2010). Enhancement of Pt and Pt-alloy fuel cell catalyst activity and durability via nitrogen-modified carbon supports. *Energy Environ. Sci* 3:1437. doi: 10.1039/c003710a

Conflict of Interest: The authors declare that the research was conducted in the absence of any commercial or financial relationships that could be construed as a potential conflict of interest.

Publisher's Note: All claims expressed in this article are solely those of the authors and do not necessarily represent those of their affiliated organizations, or those of the publisher, the editors and the reviewers. Any product that may be evaluated in this article, or claim that may be made by its manufacturer, is not guaranteed or endorsed by the publisher.